The Pugh criterion for elements in a fcc lattice

Emiel Botterman, Maarten Carrette, and Thomas Saverwyns

(Dated: 7 December 2024)

Synopsis

This project investigates the validity of the Pugh criterion for elements with an fcc crystal structure. The results show that the criterion is not universally applicable, focusing on the influence of experimental factors such as temperature and microstructure, parameters that are not accounted for in density functional theory (DFT) calculations using a single unit cell. In addition, trends in the bulk and shear moduli were analysed, revealing correlations with atomic properties, bond types and charge density distributions.

Keywords: Ductility, DFT, bulk modulus, shear modulus, Pugh criterion

I. INTRODUCTION

The mechanical behaviour of materials can be divided into two main categories. There are ductile and non-ductile materials. When increasingly more stress is applied to a non-ductile material, it will break 'suddenly' with hardly experiencing any deformation prior to the fracture. A ductile material on the other hand will undergo plastic deformation before breaking. The ductility of materials can be determined by performing a tensile test on them. However, this can also be done in other ways. In this project, the ductility of certain elements in a face-centered cubic (fcc) lattice were researched using density functional theory (DFT). The advantage of DFT in this context is that elements that do not exist in an fcc lattice can be created and tested in this way. During this project the software that was used for the calculations was Quantum Espresso (QE) [3][5][4]. For all materials, the Perdew-Burke-Ernzerhof (PBE) approximation for the exchange-correlation functional was used.

The goal of this project was to determine the ductility of elements in a fcc lattice for the entire periodic table. The ductility of an element can be tested by the Pugh criterion [26]. It states: a metal is expected to be ductile if $B/G > 1.75$, $G/B < 0.57$ or $\nu < 0.26$. B is the bulk modulus of a material, G the shear modulus and ν the Poisson's ratio. Those values could be determined using DFT. In this project B/G was determined for: Th, K, W, Si, I and some additional elements. These results will be compared to experimental ductility information to see whether the Pugh criterion holds. Finally, trends in the B/G ratio across the Periodic System of Elements (PSE) will be examined and a possible explanation was formulated.

II. METHOD

As mentioned in the introduction to determine whether or not a material violates the Pugh criterion, a need arises to calculate the bulk modulus and the shear modulus. In this project the bulk moduli were calculated with two different methods. One method was calculating the total energies of different volumes for each of the materials and fitting to the equations of states (EOS), this was also needed to find the optimal volume of the unit cell. The second method was by first calculating the elastic constants by using the stress tensor. The shear moduli were calculated only from the elastic constant method. A more thorough explanation of these two methods is given in appendix II.

III. RESULTS AND COMPARISON

The results from the convergence testing are given in table I together with the computed volume of the unit cell, bulk modulus and comparisons with FLEUR and WIEN2k. For each element three separate convergence tests were done. The parameters of the best performing one were selected. For the elements Si, K and I there is a close to excellent match between the results from Quantum Espresso and the other codes. For all elements, a smaller volume for the unit cell was found, but the relative differences in bulk moduli are smaller than 3%.

For W and Th, there is a poor match between the different codes. In these heavy elements, spin-orbit coupling becomes important. This interaction is not encoded in the used X.pbe-spn-kjpaw_psl.1.0.0.UPF pseudopotentials. These pseudopotentials are called 'scalar relativistic' because there is no spin-orbit coupling. WIEN2k and FLEUR are all-electron codes and have spin-orbit coupling. For this reason, also a 'full relativistic' pseudopotential has been used for tungsten of the type W.rel-pbe-spn-kjpaw_psl.1.0.0.UPF. With this relativistic pseudopotential a much better fit was obtained. The volume of the unit cell found with this pseudopotential is much closer to the volume found in the literature [1], but the bulk modulus calculated with this pseudopotential was further off compared to the scalar relativistic pseudopotential. For this reason also the shear modulus was calculated with the scalar relativistic pseudopotential and further computations were done for only light atoms.

TABLE I: Convergence testing results and comparison with literature values for different elements [1]. The result for W in a separate box was obtained using the full relativistic pseudopotential.

Element	**Parameters**	V_0 ($\AA^3$)	B_0 (GPa)	B_1	ν **FLEUR-QE**	ν **WIEN2k-QE**
Si	k-mesh: 35x35x35 ecutwft: 90 ecutrho: 180	14.47	84.0	4.28	0.1281	0.08995
K	k-mesh: 15x15x15 ecutwft: 90 ecutrho: 360	73.93	3.6	3.77	0.129794	0.13115
I	k-mesh: 35x35x35 ecutwft: 70 ecutrho: 210	35.03	23.9	5.55	0.20612	0.211672
W	k-mesh: 35x35x35 ecutwft: 70 ecutrho: 280	16.37	282.6	4.00	0.54785	0.524277
Th	k-mesh: 20x20x20 ecutwft: 120 ecutrho: 600	32.01	56.3	3.92	0.5414	0.5686
W	k-mesh: 20x20x20 ecutwft: 70 ecutrho: 280	16.44	275.9	3.94	0.1508	0.1316

For each element in their fcc state, the bulk-and shear modulus were calculated using the stress tensor method (STM). The results are shown in table II. The values of B/G were compared to computed values from values obtained from [14]. For the five major elements of this work, there is always a slight overestimation for calculated B/G in comparison with the literature. However, the differences are not significant and the conclusions using Pugh criterion will be the same. The same comparison was made for the other calculated elements. Here, the results were similar to those of the literature. Only for Al and V there was a larger difference. To confirm Pugh's criterion, experimental data is needed. B/G was experimentally determined for most of the elements at 0K. Most of them were not in a fcc

lattice, as that state is unstable for those materials. Therefore, the differences in calculated and experimental results are large. From the main elements of this work, only thorium exists in a fcc lattice. Other calculated elements existing in a fcc lattice are: Al, Ca and Co. The calculated and experimental results for fcc lattice materials are similar, except for Co. The Pugh criterion predicts Co to be non-ductile when B/G is calculated. However experiments show that Co is ductile.

Experimental results of ductility are needed for the validation of the Pugh criterion. The value of elongation before fracture is used to express ductility. The ductility of a material becomes larger when this value increases. When the fracture elongation is low, the material is non-ductile. It is difficult to find experimental data for ductility of single atom materials. The few results found, need to be analysed critically. Most of the tests were performed on materials that are not in an fcc lattice structure. Moreover, the conditions in which the experiments are done differ. Meaning that some experiments were done at different temperatures than 0K, and DFT calculations assume the structures to be at 0K. Mechanical properties are dependent of temperature, pre-testing treatments, microstructure of the material (grain size), testing conditions. Those are not equal for all the tested elements. This makes it difficult to draw an overall conclusion about the Pugh criterion.

From the five major elements of this work, I is the only element for which no experimental values were found. For the other elements, the calculated B/G using STM (fcc) will be compared to the experimental elongation (specific structure per element). According to the Pugh criterion, a material will be ductile when $B/G > 1.75$. Si and K can be considered ductile according to the elongation. Their calculated values for B/G are significantly higher than 1.75. However, the results for W and Th contradict Pugh's criterion. Th has a high experimental ductility and a low B/G-ratio. W, on the other hand, is clearly non-ductile, but has a calculated B/G-ratio that is slightly higher than 1.75. The results that should be the most accurate are those where the experimental results are also coming from an fcc lattice. The experimental results show that Co and Al are ductile materials. Also Ca can be considered to be ductile as well, but less than Co and Al. The Pugh criterion holds for Al and Ca, but with Co the same result as with Th can be observed. From four fcc materials researched, only two follow Pugh's criterion.

Many experimental ductility values were determined on body-centered cubic (bcc) (Im3m) structured materials. fcc materials tend to be more ductile than bcc, because bcc has a more closed packed structure [22]. The calculated values for B/G in fcc are generally higher than those in bcc. Therefore, the Pugh criterion for fcc materials cannot be confirmed by experimental data from bcc. For Na, Cr and W B/G for fcc is slightly higher than 1.75. According Pugh's criterion, the materials should be ductile, but when tested in bcc, they are non-ductile. However for V in an fcc structure, B/G is significantly higher than 1.75. In this case, the tested bcc material is ductile.

IV. TRENDS IN THE PSE

To find trends in the B/G ratio across the PSE, it may be easier to find trends in the different moduli separately. First, the bulk modulus is investigated. Figure 1 shows the values for the bulk modulus of elements in an fcc structure up to Xe. These values were obtained from [1]. In the same period, the bulk modulus decreases for heavier elements. This is directly related to the charge density and is shown in figure 4. This figure shows the difference in charge density for Na and K. Both graphs are similar because they are below each other in the same column, but the values are different. The charge density between atoms is greater for Na compared to K, therefore it will be more difficult to compress or expand the unit cell. This results in a larger bulk modulus. However, this is not the full

TABLE II: Results of calculated (STM) and literature (lit) values of B and G for different elements in fcc. Experemantal (exp) values for B/G and elongation of different elements are given in their stable space group.

Element	B_0 (GPa)(STM)	G (GPa)(STM)	B/G (STM)	B/G (lit)	B/G (exp)	**elong** (%)(exp)	**Space group** (exp)
Si	83.08	18.33	4.53	3.72[14]	1.44[8]	30.0[29]	Fd3m1[14]
K	3.55	1.32[30]	2.69	2.00[14]	1.96[30]	12.0[10]	Im3m[14]
I	23.98	2.97	8.07	/	/	/	Cmce[14]
W	283.26	153.79	1.84	1.62[14]	1.92[30]	> 1[27]	Im3m[14]
Th	55.19	39.89	1.38	1.25[14]	1.58[30]	34[23]	Fm3m[14]
Na	6.61	2.75	2.41	/	1.94[30]	2.00[23]	Im3m[14]
Al	77.00	31.69	2.44	4.28[14]	2.70[30]	11.8[2]	Fm3m[14]
Ca	17.36	9.62	1.80	1.89[14]	1.83[9]	7.0[23]	Fm3m[14]
Sc	51.60	24.53	2.10	2.13[14]	1.73[17]	5.0[23]	$P6_3/mmc$[14]
Ti	106.85	40.45	2.64	2.53[14]	2.21[12]	24.0[24]	P6/mmm[14]
V	175.50	36.53	4.80	3.61[14]	3.25[11]	13.0[31]	Im3m[14]
Cr	236.80	115.74	2.05	1.86[14]	1.41[30]	> 1[23]	Im3m[14]
Co	260.23	175.62	1.48	1.58[14]	2.01[28]	19.0[15]	Fm3m[14]
Zn	84.01	6.78	12.40	/	1.80[16]	4.8[32]	$P6_3/mmc$[14]
Br	28.56	20.98	1.36	1.45[14]	/	/	Cmce[14]
Rb	2.76	1.18	2.34	3.00[14]	2.24[30]	/	Im3m[14]

explanation because the central transition metals have an increasing bulk modulus going down a period. An atomic property that has the same trends, is the electronegativity. The bulk modulus will thus be dependent on the charge density and the electronegativity [20][7][25][6][21].

For elements in the same row, a trend across the row is not so clear. For the d-block elements, the value for the bulk modulus goes up and down almost symmetrically. A similar trend applies to the unit cell volume going down and up again. This affects the charge density and hence the bulk modulus. A similar evolution in bulk modulus happens for the p-block elements with the exception of B which has an exceptional small volume. However, this trend cannot be linked to volume since Ge has a larger volume but a larger bulk modulus compared to Ga. To better understand the evolution of the bulk modulus, it is necessary to split it into a contribution of the volume, electronegativity and charge density and study these contributions separately [18].

The next step is to look for trends in the shear modulus. As the bulk modulus decreases for elements in the same period, the shear modulus for the alkali metals was calculated to find a similar pattern. The same trend holds for these elements and the shear modulus becomes smaller for heavier elements. Similar findings apply for Cl/ Br. The opposite was found for Cr/W, just as for the bulk modulus. This suggests that the same trends in a period hold for the shear modulus and the bulk modulus. Again, this could be related to the charge density and electronegativity.

For d-block elements in the same row, there is a clear trend visible. The absolute value of the shear modulus becomes larger for elements up to Co and than drops quickly. Looking at the charge density difference plots in fig 5, a similar trend is present in the spacial dependence of the charge density difference. The plots become more and more rotationally asymmetric up to Co. For Zn, the plot resembles the Na or K plots, fig 4, and is almost rotationally symmetric. The shear modulus is a measure on how easy the atoms can slide on top of each other. If the electron density between atoms stays constant, this will happen easily. However, if there is a significant charge build-up, the atoms are more repelled and the shear modulus will be bigger. This suggest that the type of bond plays an important factor in the value of the shear modulus. On the other hand, the valence central charge

density between atoms goes up until Fe and then drops again [19].

The p-block elements have not been tested as extensively as the d-block elements. The bonding character of these elements is more covalent like and thus also more directional. From above one would expect high values for the shear modulus. However, the opposite is true and is explained using I. In fig 6, the charge density and charge density difference is given. The central charge density is extremely low. Hence it is energetically favourable for the atoms to move to that spot as the electronic repulsion would be less. This is also visible in the charge density difference plot. The central charge density difference is slightly negative. This means that it looks like an attractive potential and the atoms want to slide towards this potential. This is why the shear modulus was found to be negative for I in a fcc lattice. The reason for this smallness is probably a combination of the directional bond and the smallness of the central charge density difference.

Combining the trends of the bulk modulus and the shear modulus, it is possible to state trends in the B/G ratio. Going down a period, both moduli go down, but not at the same rate. This results in a B/G ratio that is not predictable. For the d-block elements, the bulk modulus goes up and down almost symmetrically, but the shear modulus goes up to Co after which it drops drastic. This results in a B/G ratio that grows up to V, becomes smaller up to Co and then rapidly grows for the remaining elements. For the p-block elements, the bulk modulus goes up and down and it is guessed that the bulk modulus becomes smaller. This results in a B/G ratio that increases. In order to have a complete understanding, further investigation is needed on why the electronic densities behave as they do.

V. CONCLUSION

Comparing the B/G ratio's, and evaluating the Pugh criterion, with the elongation, it is hard to obtain a certain conclusion about ductility properties of the tested materials. The primary reason for this is that the experimental values of fracture elongation do not represent the general ductility of the material. The tests were performed at different temperatures and the materials had specific microstructures. These factors have a great impact on the ductility of a material. To get more representative results, each material should be tested at the same temperature and should have a similar microstructure.

In future work it may be interesting to look for a link between fcc and bcc structures. From which calculated value of B/G in fcc is the bcc material ductile? When the bcc variant of a material is ductile, does that imply fcc is ductile as well?

Further, trends in the bulkmodulus, shearmodulus and the B/G ratio were looked into. It was found that both moduli decrease in a period and this is related to the decrease in charge density. For the central transition metals, the opposite holds and could be related to an increase in electronegativity. This results in a non trivial trend in their respective ratio. The p-block elements were not investigated extensively so no trends could be observed. For the transition metals, the bulkmodulus and shearmodulus have different behaviour. This results in a growing ratio because the bulkmodulus increases. Then the ratio becomes smaller, as the bulkmodulus decreases and the shearmodulus increases. Finally the ratio goes up again because the shearmodulus drops quickly. It was found that Zn has the highest B/G ratio and would have the longest elongation according to the Pugh criterion.

REFERENCES

[1] Emanuele Bosoni et al. "How to verify the precision of density-functional-theory implementations via reproducible and universal workflows". In: *Nature Reviews Physics* 6.1 (Nov. 2023), pp. 45–58. ISSN: 2522-5820. DOI: 10.1038/s42254-023-00655-3. URL: http://dx.doi.org/10.1038/s42254-023-00655-3.

[2] Zhaohe Gao et al. "Effects of minor Zr and Er on microstructure and mechanical properties of pure aluminum". In: *Materials Science and Engineering: A* 580 (2013), pp. 92–98. ISSN: 0921-5093. DOI: 10.1016/j.msea.2013.05.035. URL: https://www.sciencedirect.com/science/article/pii/S0921509313005650.

[3] P Giannozzi et al. "Advanced capabilities for materials modelling with QUANTUM ESPRESSO". In: *Journal of Physics: Condensed Matter* 29.46 (2017), p. 465901. URL: http://stacks.iop.org/0953-8984/29/i=46/a=465901.

[4] Paolo Giannozzi et al. "Quantum ESPRESSO toward the exascale". In: *The Journal of Chemical Physics* 152.15 (2020), p. 154105. DOI: 10.1063/5.0005082. eprint: https://doi.org/10.1063/5.0005082. URL: https://doi.org/10.1063/5.0005082.

[5] Paolo Giannozzi et al. "QUANTUM ESPRESSO: a modular and open-source software project for quantum simulations of materials". In: *Journal of Physics: Condensed Matter* 21.39 (2009), 395502 (19pp). URL: http://www.quantum-espresso.org.

[6] Zelong Gong et al. "Young's modulus prediction model for metal carbides based on first-principles calculations". In: *Materials Chemistry and Physics* 307 (2023), p. 128137. ISSN: 0254-0584. DOI: https://doi.org/10.1016/j.matchemphys.2023.128137. URL: https://www.sciencedirect.com/science/article/pii/S0254058423008453.

[7] Sanjay Kumar Gorai. "Estimation of Bulk modulus and microhardness of tetrahedral semiconductors". In: *Journal of Physics: Conference Series* 365.1 (May 2012), p. 012013. DOI: 10.1088/1742-6596/365/1/012013. URL: https://dx.doi.org/10.1088/1742-6596/365/1/012013.

[8] John J. Hall. "Electronic Effects in the Elastic Constants of n-Type Silicon". In: *Phys. Rev.* 161 (3 Sept. 1967), pp. 756–761. DOI: 10.1103/PhysRev.161.756. URL: https://link.aps.org/doi/10.1103/PhysRev.161.756.

[9] Jason E. Hearn et al. "Global potentials for calcium and strontium solids". In: *J. Chem. Soc., Faraday Trans.* 92 (3 1996), pp. 425–432. DOI: 10.1039/FT9969200425. URL: http://dx.doi.org/10.1039/FT9969200425.

[10] D. Hull and H. M. Rosenberg. "The deformation of lithium, sodium and potassium at low temperatures: Tensile and resistivity experiments". In: *The Philosophical Magazine: A Journal of Theoretical Experimental and Applied Physics* 4.39 (1959), pp. 303–315. DOI: 10.1080/14786435908233342. eprint: https://doi.org/10.1080/14786435908233342. URL: https://doi.org/10.1080/14786435908233342.

[11] Hideaki Ikehata et al. "First-principles calculations for development of low elastic modulus Ti alloys". In: *Phys. Rev. B* 70 (17 Nov. 2004), p. 174113. DOI: 10.1103/PhysRevB.70.174113. URL: https://link.aps.org/doi/10.1103/PhysRevB.70.174113.

[12] Hideaki Ikehata et al. "First-principles calculations for development of low elastic modulus Ti alloys". In: *Phys. Rev. B* 70 (17 Nov. 2004), p. 174113. DOI: 10.1103/PhysRevB.70.174113. URL: https://link.aps.org/doi/10.1103/PhysRevB.70.174113.

[13] Mahmoud Jafari et al. "Pseudopotential calculation of the bulk modulus and phonon dispersion of the bcc and hcp structures of titanium". In: *Physica Scripta - PHYS SCR* 83 (June 2011). DOI: 10.1088/0031-8949/83/06/065603.

[14] Anubhav Jain et al. "Commentary: The Materials Project: A materials genome approach to accelerating materials innovation". In: *APL Materials* 1.1 (July 2013), p. 011002. ISSN: 2166-532X. DOI: 10.1063/1.4812323. eprint: https://pubs.aip.org/aip/apm/article-pdf/doi/10.1063/1.4812323/13163869/011002_1_online.pdf. URL: https://doi.org/10.1063/1.4812323.

[15] Amir A. Karimpoor and Uwe Erb. "Mechanical properties of nanocrystalline cobalt". In: *physica status solidi (a)* 203.6 (2006), pp. 1265–1270. DOI: https://doi.org/10.1002/pssa.200566157. eprint: https://onlinelibrary.wiley.com/doi/pdf/10.1002/pssa.200566157. URL: https://onlinelibrary.wiley.com/doi/abs/10.1002/pssa.200566157.

[16] H. M. Ledbetter. "Elastic properties of zinc: A compilation and a review". In: *Journal of Physical and Chemical Reference Data* 6.4 (Oct. 1977), pp. 1181–1203. ISSN: 0047-2689. DOI: 10.1063/1.555564. eprint: https://pubs.aip.org/aip/jpr/article-pdf/6/4/1181/11494948/1181_1_online.pdf. URL: https://doi.org/10.1063/1.555564.

[17] R. G. Leisure et al. "Room-temperature elastic constants of Sc and $ScD_{0.18}$". In: *Phys. Rev. B* 48 (2 July 1993), pp. 1276–1279. DOI: 10.1103/PhysRevB.48.1276. URL: https://link.aps.org/doi/10.1103/PhysRevB.48.1276.

[18] J T Lenkkeri. "The elastic moduli of face-centred cubic transition metal alloys". In: *Journal of Physics F: Metal Physics* 11.10 (Oct. 1981), p. 1997. DOI: 10.1088/0305-4608/11/10/009. URL: https://dx.doi.org/10.1088/0305-4608/11/10/009.

[19] Chengbin Li et al. "First principles study on the charge density and the bulk modulus of the transition metals and their carbides and nitrides". In: *Chinese Physics - CHIN PHYS* 14 (Nov. 2005), pp. 2287–2292. DOI: 10.1088/1009-1963/14/11/024.

[20] Keyan Li, Zhongsheng Ding, and Dongfeng Xue. "Electronegativity-related bulk moduli of crystal materials". In: *physica status solidi (b)* 248.5 (2011), pp. 1227–1236. DOI: https://doi.org/10.1002/pssb.201046448. eprint: https://onlinelibrary.wiley.com/doi/pdf/10.1002/pssb.201046448. URL: https://onlinelibrary.wiley.com/doi/abs/10.1002/pssb.201046448.

[21] Keyan Li and Dongfeng Xue. "Empirical calculations of elastic moduli of crystal materials". In: *Physica Scripta* 2010.T139 (May 2010), p. 014072. DOI: 10.1088/0031-8949/2010/T139/014072. URL: https://dx.doi.org/10.1088/0031-8949/2010/T139/014072.

[22] S.J. Lim and H. Huh. "Ductile fracture behavior of BCC and FCC metals at a wide range of strain rates". In: *International Journal of Impact Engineering* 159 (2022), p. 104050. ISSN: 0734-743X. DOI: https://doi.org/10.1016/j.ijimpeng.2021.104050. URL: https://www.sciencedirect.com/science/article/pii/S0734743X21002372.

[23] MatWeb LLC. "MatWeb: Online Materials Information Resource". In: *MatWeb* 1.1 (1996-2024). URL: https://www.matweb.com/.

[24] Michael McCracken. "Dental Implant Materials: Commercially Pure Titanium and Titanium Alloys". In: *Journal of Prosthodontics* 8.1 (1999), pp. 40–43. DOI: https://doi.org/10.1111/j.1532-849X.1999.tb00006.x. eprint: https://onlinelibrary.wiley.com/doi/pdf/10.1111/j.1532-849X.1999.tb00006.x. URL: https://onlinelibrary.wiley.com/doi/abs/10.1111/j.1532-849X.1999.tb00006.x.

[25] Author-Shiv Om Kumar, Vineeta Shukla, and Sanjeev Kumar Srivastava. "Role of electronegativity on the bulk modulus, magnetic moment and band gap of Co2MnAl based Heusler alloys". In: *Journal of Science: Advanced Materials and Devices* 4.1 (2019), pp. 158–162. ISSN: 2468-2179. DOI: https://doi.org/10.1016/j.jsamd.2019.02.001. URL: https://www.sciencedirect.com/science/article/pii/S2468217919300048.

[26] S.F. Pugh. "XCII. Relations between the elastic moduli and the plastic properties of polycrystalline pure metals". In: *The London, Edinburgh, and Dublin Philosophical Magazine and Journal of Science* 45.367 (1954), pp. 823–843. DOI: 10.1080/14786440808520496. eprint: https://doi.org/10.1080/14786440808520496. URL: https://doi.org/10.1080/14786440808520496.

[27] Chai Ren et al. "Methods for improving ductility of tungsten - A review". In: *International Journal of Refractory Metals and Hard Materials* 75 (2018), pp. 170–183. ISSN: 0263-4368. DOI: https://doi.org/10.1016/j.ijrmhm.2018.04.012. URL: https://www.sciencedirect.com/science/article/pii/S0263436818300659.

[28] S. Subramanian et al. "Elastic constants of body-centered-cubic cobalt films". In: *Phys. Rev. B* 49 (24 June 1994), pp. 17319–17324. DOI: 10.1103/PhysRevB.49.17319. URL: https://link.aps.org/doi/10.1103/PhysRevB.49.17319.

[29] W. D. Sylwestrowicz. "Mechanical properties of single crystals of silicon". In: *The Philosophical Magazine: A Journal of Theoretical Experimental and Applied Physics* 7.83 (1962), pp. 1825–1845. DOI: 10.1080/14786436208213849. eprint: https://doi.org/10.1080/14786436208213849. URL: https://doi.org/10.1080/14786436208213849.

[30] K P Thakur. "Mechanical behaviour of FCC and BCC metals and their stability under hydrostatic compressive and tensile stresses". In: *Journal of Physics F: Metal Physics* 15.12 (Dec. 1985), p. 2421. DOI: 10.1088/0305-4608/15/12/005. URL: https://dx.doi.org/10.1088/0305-4608/15/12/005.

[31] R.H. van Fossen, T.E. Scott, and O.N. Carlson. "The effect of strain rate and temperature on the ductility of pure and hydrogenated vanadium". In: *Journal of the Less Common Metals* 9.6 (1965), pp. 437–451. ISSN: 0022-5088. DOI: https://doi.org/10.1016/0022-5088(65)90128-1. URL: https://www.sciencedirect.com/science/article/pii/0022508865901281.

[32] Chengzhe Wang et al. "Microstructural evolution and mechanical properties of pure Zn fabricated by selective laser melting". In: *Materials Science and Engineering: A* 846 (2022), p. 143276. ISSN: 0921-5093. DOI: https://doi.org/10.1016/j.msea.2022.143276. URL: https://www.sciencedirect.com/science/article/pii/S0921509322006761.

Appendix A: Supplementary tables and figures

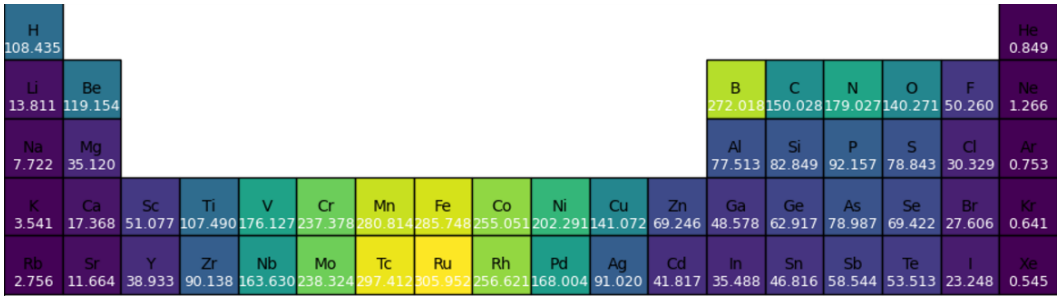

FIG. 1: Bulk moduli (GPa) for elements up to Xe in the fcc structure obtained from [1]. Clear trends are visible in the same column of the PSE.

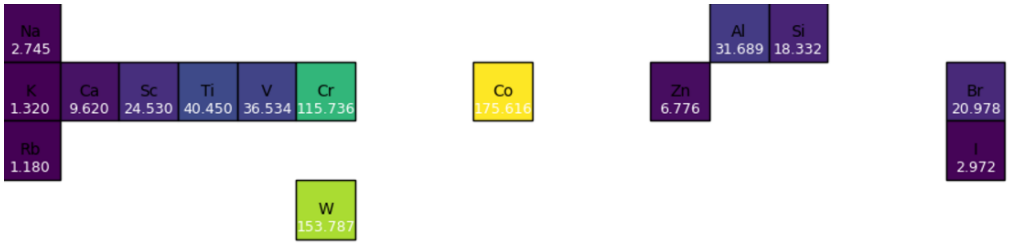

FIG. 2: Computed absolute value of the shear moduli (GPa) for elements up in the fcc structure.

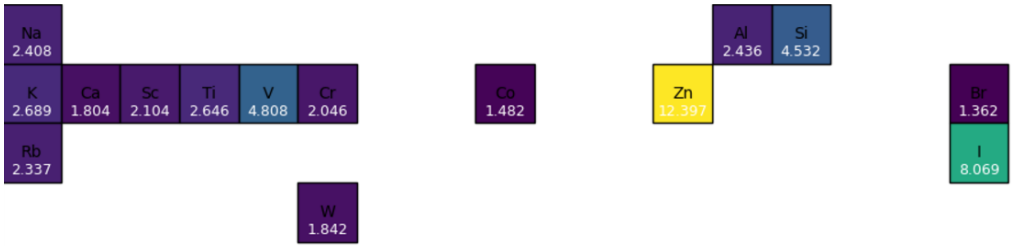

FIG. 3: Computed B/G ratio for elements in the fcc structure.

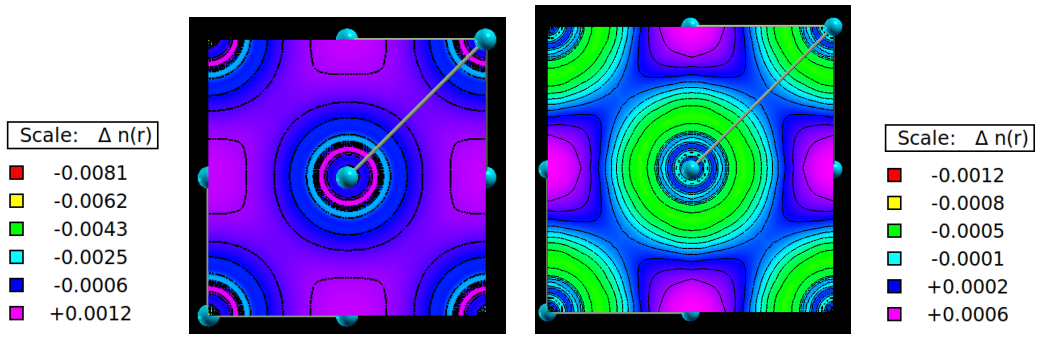

FIG. 4: Charge density difference with legend. The central charge density between atoms for K is smaller compared to Na. This results in a smaller bulk modulus. Left: Na, Right:K

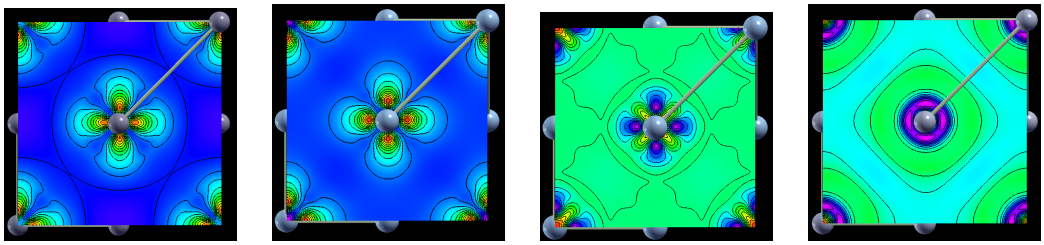

FIG. 5: Charge density difference for the elements Ti, Cr, Co and Zn. The charge density difference plots become more and more rotationally asymmetric up to Co. This results in a increasing shearmodulus.

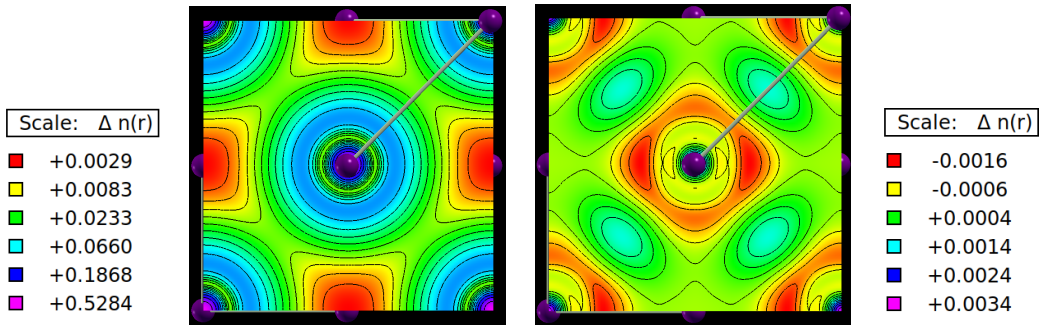

FIG. 6: Left: Charge density plot for I with legend. The central charge density is extremely low. Right: Charge density difference plot for I with legend. Strong directional bonds are visible, but the central density difference is slightly negative, creating almost an attractive force towards that spot.

Appendix B: Method

1. Convergence testing

When calculations are to be done on a crystal using DFT, a convergence test needs to be performed on it first. By doing this, numerically meaningful results will be calculated rather than noise. To start with convergence testing, an approximate lattice constant is needed. This value was obtained from [1]. This is needed to build an input file for a specific

element in an fcc-lattice. Each element also needs a pseudopotential. The following form for pseudopotentials: X.pbe-spn-kjpaw psl.1.0.0.UPF was used. With a complete input file, the convergence testing can begin. First, the k-mesh size was increased. For each step, the calculated pressure and runtime were noted. The lowest k-mesh size for which the fluctuation in pressure was less than 1% was accepted. After this, the ranges of the ecutwtf and ecutrho values were changed. These adaptations caused a decrease in fluctuations. Values for k-mesh, ecutwtf, and ecutrho that showed good convergence within a reasonable computation time were chosen. High k-meshes and cutoff energies were used, because the computations were done on the TIER-2 HPC from Ghent University.

TABLE III: Results from convergence testing, together with the lattice constant obtained from the EOS fit.

	a_0 (Å)	k-mesh	$E_{\text{cut,wft}}$ (Ry)	$E_{\text{cut,rho}}$ (Ry)
Na	5.29818	35x35x35	70	350
Ca	5.52727	30x30x30	70	350
Sc	4.61674	30x30x30	100	500
Ti	4.11714	30x30x30	120	800
V	3.82368	30x30x30	150	750
Cr	3.62550	30x30x30	150	1500
Rb	7.13847	30x30x30	55	330
Al	4.03753	25x25x25	60	300
Br	4.72159	35x35x35	100	500
Co	3.44587	35x35x35	100	1000
Zn	3.92451	35x35x35	100	500

2. Equation of states method

To compute the bulkmoduli, deviations in the volume up to 10% of the values from [1] were used. 6 equidistant lattice constants were used to compute the total energy and to make a fit to the Birch–Murnaghan equation of state. The fit was made using the ev.x command from Quantum Espresso. This gave values for the volume of the unit cell, bulkmodulus and the derivative of the bulkmodulus with respect to the pressure. To validate these results, comparisons were made with the results from [1]. These comparisons were done by the following definition, with weights $w_{V_0} = 1, w_{B_0} = \frac{1}{20}, w_{B_1} = \frac{1}{400}$:

$$\nu_{w_{V_0},w_{B_0},w_{B_1}}(a,b) = 100\sqrt{\sum_{Y=V_0,B_0,B_1}\left[w_Y \cdot \frac{Y_a - Y_b}{(Y_a+Y_b)/2}\right]^2}$$

Values of $\nu < 0.1$ are an excellent match between the two results and values of $\nu < 0.33$ is considered good.

3. Stress tensor method

This method uses that there is a relation between the strain tensor and the stress tensor. By using the Voight notation for the strain and the stress tensor and for a general material, i.e. no symmetry, six different deformations of the unit cell will need to be considered. These six deformations are three tensile deformations and three shear deformation. All of the deformation need to be linear independent of each other. Each deformation will lead to a specific strain tensor. These strain tensors can be calculated via the definition of the strain tensor.

$$E = \frac{1}{2}\left(F^T F - \mathbb{1}\right)$$

With F being the deformation matrix and F^T being the transposed deformation matrix, and $\mathbb{1}$ is the identity matrix.

To deform the unit cells, the deformation matrix F is multiplied with the root tensor of the material. The resulting matrix is the root tensor for the deformed unit cell. In this project Quantum Espresso is used for the calculation of the stress tensor. It is important to note that for the $CELL\_PARAMETERS$ input files used for these calculations, the root tensor needs to be transposed. Also the position of the atoms have to be optimized prior to calculating the stress tensor. The stress tensor obtained from the output of QE is the external stress. For these calculations the internal stress is needed therefore the signs of the values from the output of the QE-calculation needs to be inverted. The Voight notation for these 3x3 matrices is a column vector with six values.

$$\begin{bmatrix} \sigma_{xx} & \sigma_{xy} & \sigma_{xz} \\ \sigma_{xy} & \sigma_{yy} & \sigma_{yz} \\ \sigma_{xz} & \sigma_{yz} & \sigma_{zz} \end{bmatrix} \rightarrow \begin{bmatrix} \sigma_{xx} \\ \sigma_{yy} \\ \sigma_{zz} \\ \sigma_{yz} \\ \sigma_{xz} \\ \sigma_{xy} \end{bmatrix}$$

This is the Voight notation for the stress tensor. for the strain tensor the Voight notation is a bit different.

$$\begin{bmatrix} \epsilon_{xx} & \epsilon_{xy} & \epsilon_{xz} \\ \epsilon_{xy} & \epsilon_{yy} & \epsilon_{yz} \\ \epsilon_{xz} & \epsilon_{yz} & \epsilon_{zz} \end{bmatrix} \rightarrow \begin{bmatrix} \epsilon_{xx} \\ \epsilon_{yy} \\ \epsilon_{zz} \\ 2\epsilon_{yz} \\ 2\epsilon_{xz} \\ 2\epsilon_{xy} \end{bmatrix}$$

The relation between the stress tensor and the strain tensor is the stiffness tensor, this is a tensor with components C_{ij} which are the elastic constants. From these elastic constants properties of materials can be calculated.

$$\begin{bmatrix} \sigma_{xx} \\ \sigma_{yy} \\ \sigma_{zz} \\ \sigma_{yz} \\ \sigma_{xz} \\ \sigma_{xy} \end{bmatrix} = \begin{bmatrix} C_{11} & C_{12} & C_{13} & C_{14} & C_{15} & C_{16} \\ C_{12} & C_{22} & C_{23} & C_{24} & C_{25} & C_{26} \\ C_{13} & C_{23} & C_{33} & C_{34} & C_{35} & C_{36} \\ C_{14} & C_{24} & C_{34} & C_{44} & C_{45} & C_{46} \\ C_{15} & C_{25} & C_{35} & C_{45} & C_{55} & C_{56} \\ C_{16} & C_{26} & C_{36} & C_{46} & C_{56} & C_{66} \end{bmatrix} \begin{bmatrix} \epsilon_{xx} \\ \epsilon_{yy} \\ \epsilon_{zz} \\ 2\epsilon_{yz} \\ 2\epsilon_{xz} \\ 2\epsilon_{xy} \end{bmatrix}$$

For six deformations the equations can be written as the following.

$$\begin{bmatrix} \sigma_{11} & \sigma_{12} & \sigma_{13} & \sigma_{14} & \sigma_{15} & \sigma_{16} \\ \sigma_{21} & \sigma_{22} & \sigma_{23} & \sigma_{24} & \sigma_{25} & \sigma_{26} \\ \sigma_{31} & \sigma_{32} & \sigma_{33} & \sigma_{34} & \sigma_{35} & \sigma_{36} \\ \sigma_{41} & \sigma_{42} & \sigma_{43} & \sigma_{44} & \sigma_{45} & \sigma_{46} \\ \sigma_{51} & \sigma_{52} & \sigma_{53} & \sigma_{54} & \sigma_{55} & \sigma_{56} \\ \sigma_{61} & \sigma_{62} & \sigma_{63} & \sigma_{64} & \sigma_{65} & \sigma_{66} \end{bmatrix} = \begin{bmatrix} C_{11} & C_{12} & C_{13} & C_{14} & C_{15} & C_{16} \\ C_{12} & C_{22} & C_{23} & C_{24} & C_{25} & C_{26} \\ C_{13} & C_{23} & C_{33} & C_{34} & C_{35} & C_{36} \\ C_{14} & C_{24} & C_{34} & C_{44} & C_{45} & C_{46} \\ C_{15} & C_{25} & C_{35} & C_{45} & C_{55} & C_{56} \\ C_{16} & C_{26} & C_{36} & C_{46} & C_{56} & C_{66} \end{bmatrix} \begin{bmatrix} \epsilon_{11} & \epsilon_{12} & \epsilon_{13} & \epsilon_{14} & \epsilon_{15} & \epsilon_{16} \\ \epsilon_{21} & \epsilon_{22} & \epsilon_{23} & \epsilon_{24} & \epsilon_{25} & \epsilon_{26} \\ \epsilon_{31} & \epsilon_{32} & \epsilon_{33} & \epsilon_{34} & \epsilon_{35} & \epsilon_{36} \\ 2\epsilon_{41} & 2\epsilon_{42} & 2\epsilon_{43} & 2\epsilon_{44} & 2\epsilon_{45} & 2\epsilon_{46} \\ 2\epsilon_{51} & 2\epsilon_{52} & 2\epsilon_{53} & 2\epsilon_{54} & 2\epsilon_{55} & 2\epsilon_{56} \\ 2\epsilon_{61} & 2\epsilon_{62} & 2\epsilon_{63} & 2\epsilon_{64} & 2\epsilon_{65} & 2\epsilon_{66} \end{bmatrix}$$

This is a systems of equations that can be solved. The large stress tensor will be Σ and the large strain tensor is E. The matrix with the elastic constants is C. The system of

equations can be written as $\Sigma = CE$. To find the elastic constants you can multiply both sides to the right with the inverse large strain tensor E^{-1}.

$$C = \Sigma E^{-1}$$

This is the method for a general material, but in this project all the materials that will be researched are in the fcc structure. In the fcc structure there is a lot of symmetry. Considering these symmetry properties will make clear that only two deformations are needed: one shear deformation and a tensile deformation. Also the only elastic constant different from zero are the C_{11}, C_{12} and C_{44}. The stiffness tensor for a cubic material is:

$$\begin{bmatrix} C_{11} & C_{12} & C_{12} & 0 & 0 & 0 \\ C_{12} & C_{11} & C_{12} & 0 & 0 & 0 \\ C_{12} & C_{12} & C_{11} & 0 & 0 & 0 \\ 0 & 0 & 0 & C_{44} & 0 & 0 \\ 0 & 0 & 0 & 0 & C_{44} & 0 \\ 0 & 0 & 0 & 0 & 0 & C_{44} \end{bmatrix}$$

From these three elastic constant both the bulk modulus and shear modulus can be calculated with the following formulas.

$$B = \frac{C_{11} + 2\,C_{12}}{3}$$
$$G = \frac{C_{11} - C_{12} + 3\,C_{44}}{5}$$

Previous formulas are used to calculate B and G in a cubic lattice. In this project, there are materials that are in a hexagonal lattice. For those, another formula is used to calculate B [13]. For the calculation of G, there is no exact formula. There are some conventions to get an approximation. In this project, the convention of following source is used [16].

$$B_{hex} = \frac{2\,(C_{11} + C_{12} + 2\,C_{13} + 1/2\,C_{33})}{9}$$
$$C = (C_{11} + C_{12})C_{33} \; - 2\,C_{13}^2$$
$$G_{hex} = (\frac{C_{44}^2\,(C_{11} - C_{12})^2 C}{24 B_{hex}})^{1/5}$$